Supporting Information

Strong underwater adhesion of injectable hydrogels triggered by diffusion of small molecules

Xing Su, ‡ [a] Wenyue Xie, ‡ [a] Pudi Wang,[a] Zhuoling Tian,[a,b] Hao Wang,[a] Zuoying Yuan,[a] Xiaozhi Liu[c] and Jianyong Huang*[a,b]

[a] Department of Mechanics and Engineering Science, Beijing Innovation Centre for Engineering Science and Advanced Technology, College of Engineering, Peking University, Beijing 100871, China.

[b]Academy for Advanced Interdisciplinary Studies, Peking University, Beijing 100871, China

[c] Tianjin Key Laboratory of Epigenetics for Organ Development of Premature Infants, Fifth Central Hospital of Tianjin, Tianjin, 300450, China

‡ These authors contributed equally to this work.

*Email: jyhuang@pku.edu.cn; Tel: +86-10-62751879; Fax: +86-10-62753562

Contents

Experimental Sections **4**

Materials 4

Synthesis of hydrogels 4

Characterisations 4

Mechanical testing 5

Adhesive testing 5

Urea diffusion evaluation 6

Cytocompatibility testing 7

Antibacterial activity 7

Degradation testing 7

Underwater 3D printing 8

Supplementary Figures **9**

Fig. S1. FTIR spectra for G0.6-T0.6 and G0.6-T0.6-U0.12. 9

Fig. S2. SEM images for **a** G0.6-T0.6 and **b** G0.6-T0.6-U0.12. 10

Fig. S3. Weight change of G0.6-T0.6 and G0.6-T0.6-U0.12 after immersion in limited water (0.1g of gel immersed in 40 mL distilled water). The water content of G0.6-T0.6 was calculated to be 27 wt %. 10

Fig. S4. Statistical data for the mechanical properties of as-prepared G0.6-T0.6, G0.6-T0.6-U0.12 rinsed for 12 hr, and G0.6-T0.6-U0.12 immersed for 12 hr. 11

Fig. S5. Cyclic tensile test of G0.6-T0.6 to a maximum tensile strain of 5. 11

Fig. S6. The shear-thinning property of G0.6-T0.6-U0.12 at ambient temperature (25 °C). 12

Fig. S7. The loss of tea polyphenols through diffusion from G0.6-T0.6-U0.12 in water was measured, which was negligible in comparison with that of urea in this study. After 12 hr, the loss of urea molecules reached 83.6% (molar ratio). In contrast, after 7 days, the loss of TP molecules was only 1.1% (molar ratio). 12

Fig. S8. a Spatial distributions of urea (in molar concentration) on the specific cross sections at the moment of t=0.1 hr. **b** Spatial distributions of average molar concentrations on the cross sections along the long sides at different time points. **c** Spatial distributions of urea (in molar concentration) at the specific cross sections along the long sides at different time points of t= t=0, 0.01, 0.1, 1, 10 and 100 hr, respectively. 13

Fig. S9. In-air adhesion of G0.6-T0.6-U0.12 to multiple substrates. 14

Fig. S10. The 10 sec' underwater adhesive strength to porcine skin of G0.6-T0.6-U0.12 and G0.6-T0.6-U0.18. 14

Fig. S11. The representative curve for the lap-shear test on the underwater adhered porcine skin after 8 hrs' immersion in water. The measured bonding area for this test was 5×6 mm^2. The corresponding adhesive strength for this test was calculated to be 156.4 kPa. 15

Fig. S12. The tensile strength and strain at break of G0.6-T0.6-U0.12 in different time intervals after immersion. 15

Fig. S13. a The formation of the "non-adhesive interface" and the regeneration of the "adhesive interface". **Ⅰ.** The "non-adhesive interface" formed on top of a piece of porcine skin following the same method mentioned in **Fig. 4a** in the main text. **Ⅱ.** Another piece of porcine skin was pressed onto the "non-adhesive interface" for 10 sec in air. **Ⅲ.** There was no adhesion to the piece of porcine skin placed on it. **Ⅳ.** The "non-adhesive interface" was smeared with 10 μl urea solution (1 mol L^{-1}). **Ⅴ.** After 4 hr, another piece of porcine skin was pressed on the top for 10 sec under water. **Ⅵ.** Obvious underwater adhesiveness appeared, confirming the transformation of the "non-adhesive interface" into the "adhesive interface". **b** The corresponding lap-shear adhesive test was conducted and the curve was presented. 16

Fig. S14. Antibacterial properties of the G0.6-T0.6-U0.12 hydrogel against *S. aureus* or *E. coli*. 17

Fig. S15. The evaluation on the degradation of G0.6-T0.6-U0.12 in the distilled water at ambient temperature. 17

Supplementary Tables 18

Table S1. Composition of the samples 18

Table S2. Comparison of properties for the existing adhesive gels. (Note that the symbols of ' √ ' and '--' denote 'Yes' and 'No or N/A', respectively.) 19

Supplementary Videos 20

Video S1: The spatio-temporal dynamics of water-triggered urea diffusion in the G0.6-T0.6-U0.12 hydrogel sample and on the adhesion interface between the hydrogel and the porcine skin. 20

Video S2: The G0.6-T0.6 hydrogel was non-adhesive to either glass or porcine skin in water. 20

Video S3: The injectable G0.6-T0.6-U0.12 hydrogel was efficiently adhesive to either glass or porcine skin in water 20

Video S4: The formation of "non-adhesive" interface for G0.6-T0.6-U0.12 after 1 hr's immersion in water. 20

Video S5: The underwater 3D printing of G0.6-T0.6-U0.12 patterns onto glass or porcine skin 20

Video S6: The stability of the underwater 3D printed logos on glass or porcine skin against shaking and flushing. 20

Video S7: The blowing G0.6-T0.6-U0.12 hydrogel balloon by using a thin syringe needle. 20

References 20

Experimental Sections

Materials

Gelatin (GE, purity: BR) and dopamine hydrochloride (DA, purity > 98.5%) were purchased from Shanghai Yuanye Bio-Technology Co., Ltd. Tannic acid (TA, ACS reagent) was provided by Shanghai energy-chemical Co., Ltd. Tea polyphenols (TP, also named epigallocatechin gallate, chemical formula: $C_{22}H_{18}O_{11}$, purity > 98%) was supplied by Beijing Beiluo Biotechnology Co., Ltd. Potassium polyacrylate (PAAK, Mw~2000, AR grade) was purchased from Heowns Biochem. LLC. Urea, acetone, sodium chloride (NaCl), Sodium dodecyl sulphate (SDS), sodium hydroxide (NaOH) and hydrochloric acid (HCl, 37 wt %) of AR grade were bought from Beijing Tong Guang Fine Chemical Co. Ltd. Phosphate Buffer Saline (PBS, pH=7.4) and Dulbecco's Modified Eagle's medium (DMEM) were derived from Thermo Fisher Scientific. All chemicals were used as received.

Synthesis of hydrogels

GE was dissolved in distilled water at 45 ^{o}C, forming 10 wt % solution. Afterwards, the solution was cooled down to ambient temperature and then specific amount of TP was added. Under vigorous stirring and mixing by a glass rod, the G-T hydrogels gradually formed. After approximately 30 min, the derived hydrogels were taken out and rinsed with water for removing the excessive uncross-linked substances. The G-T-U hydrogels were derived by vigorously mixing specific amount of urea solid powders into the G-T hydrogels. The obtained G-T-U hydrogels were loaded into a plastic syringe and sealed for the future use. For comparison, dopamine hydrochloride (DA) and tannic acid (TA) were used for replacing TP. As for DA, the GE solution was adjusted to be basic (pH=8) for achieving polydopamine (PDA).[1] The detailed compositions of the studied materials were listed in **Table S1**.

Characterisations

A PerkinElmer Spectrum 100 spectrophotometer was used for Fourier transform infrared (FTIR) spectroscopy. The wavenumber range from 4000 to 600 cm^{-1} and the resolution of 1 cm^{-1} were adopted for each sample scanned for 16 times. Scanning electron microscopy (SEM) pictures were taken by a TESCAN MAIA3 ultra high-resolution field emission scanning electron microscope (acceleration voltage: 5 kV). The hydrogel samples were lyophilized, fractured and coated with gold. An AR-G2 Advanced Rheometer (TA Instruments) was responsible for rheological tests. The storage moduli G' and loss moduli G" were measured by the dynamic frequency sweeps in the angular frequency range from 0.1 to 100 rad s^{-1} at ambient

temperature (a fixed strain of 1%). The linear viscoelastic region was demonstrated by strain sweep tests. A parallel plate geometry was of a diameter of 20 mm and a gap of 1.0 mm between two plates. The shear-thinning property of the samples was also evaluated by steady rate sweep at ambient temperature. The viscosity of the samples was measured as a function of shear rate. The water contents of hydrogels with fixed dimensions[2] were evaluated by weighing the corresponding samples before and after dehydration. The water content of G0.6-T0.6 was calculated by $(W_g - W_d) / W_g$, where W_g represented the weight of the as-prepared hydrogel, W_d represented the weight of the dehydrated hydrogel. The weight change of hydrogels upon immersion in water were also measured by weighing the samples after different time intervals.

Mechanical testing

The tensile tests were carried out on a STS10N tensometer (Xiamen East Instrument Co. Ltd.) equipped with a 20 N load cell, at the crosshead speed of 100 mm min^{-1}. The G0.6-T0.6 hydrogel samples were hot-pressed (60 ^oC) into a rectangular shape and cut. The tested samples were with the dimensions of 20 mm×5 mm×2 mm. For the cyclic tensile tests, the maximum strain was set to be 5. The G0.6-T0.6-U0.12 hydrogel samples were also hot-pressed for making samples. Those cut G0.6-T0.6-U0.12 samples were immersed in water for post-crosslinking. Individual hydrogel sample weighing 0.1g was immersed in 40 mL distilled water after a period of time, for simulating the situation in the limited aqueous environment. Hydrogel samples were also rinsed by running distilled water (rate of flow: 5 mL s^{-1}) for simulating the case in the open water environment. For each test, at least 5 samples were tested for achieving the reasonable results.

Adhesive testing

The adhesive tests were performed following our previous mythology.[2] Apart from pressing by hand for 10 sec either in air or underwater, no other means such as varying temperature, varying pH, UV radiation and etc. were used. As for substrates, clean and smooth glass, steel and PDMS substrates without any facial treatment were cut into rectangles of 20 mm×9 mm. Wood plates were made from camphor tree. Porcine skin, muscle and heart were newly purchased from the local market. The tested biotic substrates including porcine skin, muscle and heart were fresh, without any post-treatment such as degreasing or facial liquid removal. As for underwater adhesion, each test was conducted in about 40 mL distilled water by using approximately 0.1 g of G0.6-T0.6-U0.12 hydrogel. After being pressed for 10 sec, the external pressure was removed and the samples were left alone in water for different time intervals. Different aqueous environments were also considered. For glass, adhesion was performed in

seawater, detergent (SDS, 1 wt % solution), flocculant (PAAK, 1 wt % solution) and acetone. For porcine skin, adhesion was performed in PBS, DMEM, acid (HCl, pH=6) and base (NaOH, pH=8). For each test, the actual bonding area on the adhered substrates was individually measured to ensure the accuracy of measured data. The adhered samples were lap-shear tested on the tensometer (tensile rate: 5 mm min^{-1}).

Urea diffusion evaluation

Herein, the detailed method for evaluating urea diffusion was presented. 0.8 g 4-Dimethylaminobenzaldehyde（DMAB）was dissolved in 500 ml ethyl alcohol, and then 50 mL hydrochloric acid (37.5 wt %) was added into this solution upon constant stirring. Standard urea solution of different concentrations (0 mM, 5 mM, 10 mM, 20 mM, 50 mM, 0.2 M) was prepared with distilled water. Then, standard urea solution (50 μL) and DMAB solution of the same volume were placed in a 96-well plate. The absorption value at 420 nm was measured with Multimode Microplate Reader (Varioskan LUX, Thermo Fisher) for obtaining the standard curve. As for the actual measurement, fresh porcine skin was cut into strips with the dimensions of 30 mm×9 mm. Following the identical method for the underwater adhesive testing, they were adhered by 0.1 g G0.6-T0.6-U0.12 hydrogel in water, and placed in 40 mL distilled water. After different time intervals, 50 μL of fluid was collected and transferred to 96-well plate for the further evaluation. The extract was co-incubated with DMAB solution for 5 min, and then the corresponding absorption value at 420 nm was measured. Three parallel measurements were conducted for each group in order to ensure the reliability of the measured results. The derived results were converted to the concentration of urea after different time intervals via the standard curve.

For comparison, the diffusion of tea polyphenols was also measured via the classical method of ferrous-tartrate. 1g ferrous sulphate and 5g sodium potassium tartrate were dissolved in 1L DI water to obtain the ferrous-tartrate solution. Then, standard tea polyphenols solution with different concentrations were prepared. The tea polyphenol standard solution (50 μl) was allowed to react with the equal amount of ferrous-tartrate solution in a 96-well plate. Subsequently, the absorption values at 540 nm were measured with a Multimode Microplate Reader (Varioskan LUX, Thermo Fisher) to obtain the standard curve. The as-prepared G0.6-T0.6-U0.12 hydrogel samples were placed in a certain amount of water, and the liquid medium was extracted after 12 hr, 5 days and 7 days, respectively. The measured absorption values at 540 nm were converted to the concentrations of tea polyphenols based on the standard curve.

Cytocompatibility testing

Cytocompatibility in vitro was carried out following the similar method reported previously.[2] L929 fibroblast cells (kindly granted by Prof. Qing Cai, Beijing from University of Chemical Technology) were cultured with complete RPMI medium 1640 (Giboc) containing 10% fetal bovine serum (Giboc) and 1% penicillinstreptomycin solution (Giboc) in a 5% CO_2 incubator at 37 ^oC. The tested hydrogels were washed with DPBS for 3 days. And then immersed into complete medium to make extracts and sterilized the extracts by 0.2 μm filter. The cells were treated with trypsin-EDTA (Giboc) and resuspended cells with the extracts. The cells with the density of 3×10^3 were seeded into each well (96 -well plate) and allowed to grow for 24 hr, 48 hr and 72 hr. The cytocompatibility of the hydrogels were analysed by cell counting and Live/Dead assay. Live/Dead assay was carried on 2 μM calcein AM (in DPBS) and 4 μM EthD-1 (Invitrogen) working solution was added into wells. The 96-well plate was then incubated in a 5% CO_2 incubator at 37 ^oC for 20 min. A laser scanning confocal microscope (Nikon, Japan) was used to observe the morphologies of the cells. Then, the dye solution was removed and wells were washed with DPBS. The cell was digested with trypsin-EDTA. Counted cells. For each group, 4 parallel experiments were conducted for obtaining the convincing results.

Antibacterial activity

Gram-positive *S. aureus* and Gram-negative *E. coli* were prepared by incubating overnight in an orbital shaker (150 rpm, 37 ^oC), which used to investigate the antibacterial activities of the hydrogels. After incubation, bacterial cultures were collected by centrifuging and diluting with phosphate buffer saline (PBS, pH=7.4) with a final density of 10^8 CFU/mL (OD_{600}=0.5). Then sterilised under UV for 30 min in the clean bench, the tested hydrogels were formed in the EP tube and incubated for 1 hr at 37 ^oC with PBS buffer (pH=7.4). Subsequently, the hydrogel was removed and added to the 4 mL bacterial solution (PBS, OD_{600}=0.5) for co-incubation 24 hr at 37 ^oC. After diluted the bacterium solution (treated with the hydrogels) for 10^5 times, coated on the LB agar plate and cultured in 37 ^oC for 24 hr. Quantification of the viability was conducted by Colony-Forming Unit (CFU) counting. All of the described antibacterial experiments were performed independently three times.

Degradation testing

The G0.6-T0.6-U0.12 hydrogel samples were immersed in the PBS solution to reach the fully swollen state at 37 ^oC. Afterwards, the swollen samples weighing about 0.15 g were immersed in 35 mL PBS solution at 37 ^oC, to simulate the internal environment of human body. They were under constant shaking on a rocking device for the subsequent degradation. After different

time intervals, the samples were taken out, wiped out the facial liquid, and weighed. At least 5 samples were tested in the experiments. For comparison, the degradation tests of the G0.6-T0.6-U0.12 hydrogel samples were also conducted in the distilled water according to the same method.

Underwater 3D printing

Patterns (i. e. the letters of "PKU") were designed using SolidWorks and the corresponding G-codes were generated. Then the G0.6-T0.6-U0.12 hydrogel was loaded in a medical syringe, which was connected to a threaded nozzle with certain diameter. Then the hydrogel-loaded syringe was installed onto the 3D printer (SIM Max1.0). During 3D printing, the hydrogel was extruded at a feeding rate of 500 μL min^{-1} with the extruding pressure of 0.3 MPa.[3, 4] The extruded hydrogel was directly printed onto glass or fresh porcine skin under water. The temperature of water was set to be 40 ^{o}C. The derived patterns on glass or porcine skin were subsequently treated by shaking and flushing for evaluating the underwater stability.

Supplementary Figures

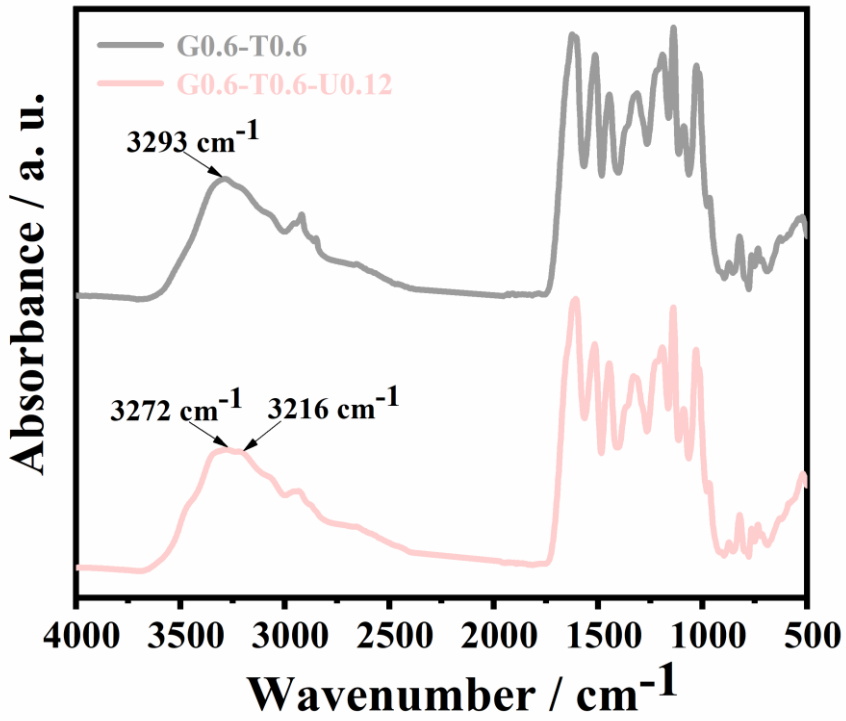

Fig. S1. FTIR spectra for G0.6-T0.6 and G0.6-T0.6-U0.12.

As shown in **Fig. S1**, the peak at 3293 cm^{-1} was characteristic for overlapped amine and hydroxyl groups in gelatin for G0.6-T0.6.[5, 6] This peak shifted to smaller wavenumber for G0.6-T0.6-U0.12, which was indicative of the dissociation of gelatin-tea polyphenol hydrogen bonds via urea.[7-9] Besides, comparing G0.6-T0.6 and G0.6-T0.6-U0.12, the intensity of the peak at 3216 cm^{-1} was higher for the latter one. This phenomenon further proved the increasing amount of liberated pyrogallol groups of TP by urea.[10-12]

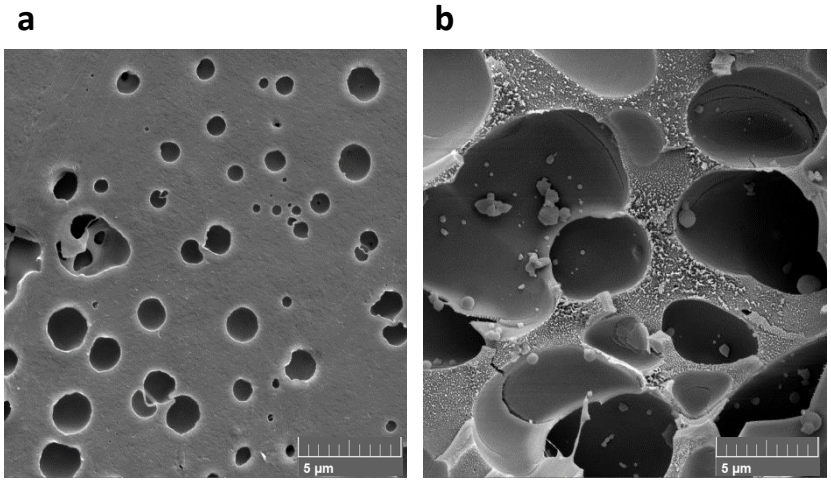

Fig. S2. SEM images for **a** G0.6-T0.6 and **b** G0.6-T0.6-U0.12.

In **Fig. S2**, comparing to G0.6-T0.6, the significantly increased pore size for G0.6-T0.6-U0.12 was due to the dissociation of hydrogen bonding crosslinking via the incorporation of urea.[13-15]

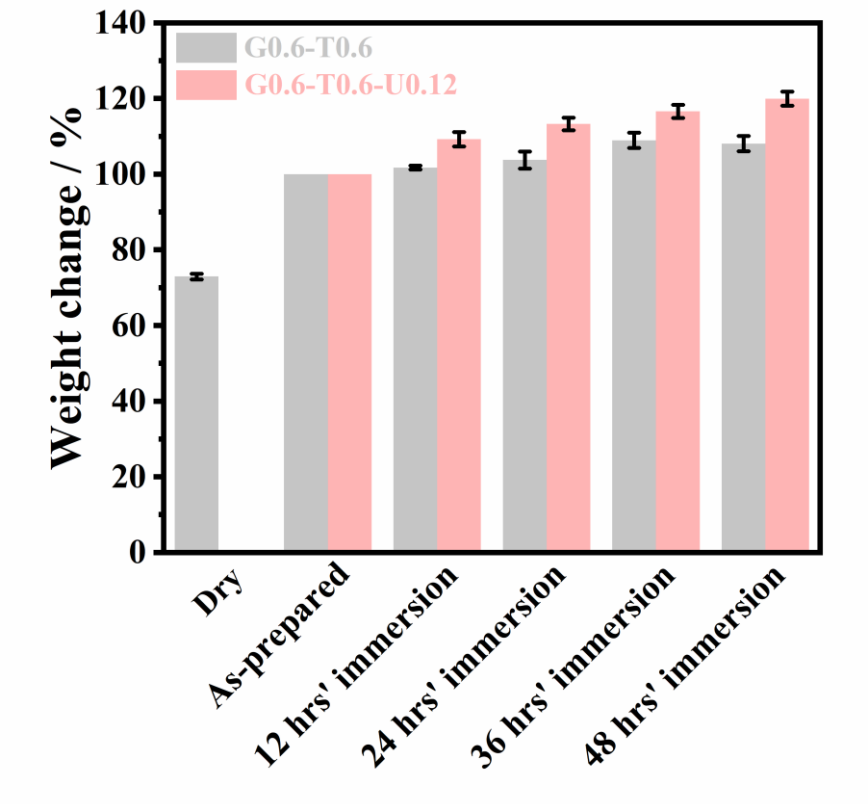

Fig. S3. Weight change of G0.6-T0.6 and G0.6-T0.6-U0.12 after immersion in limited water (0.1g of gel immersed in 40 mL distilled water). The water content of G0.6-T0.6 was calculated to be 27 wt %.

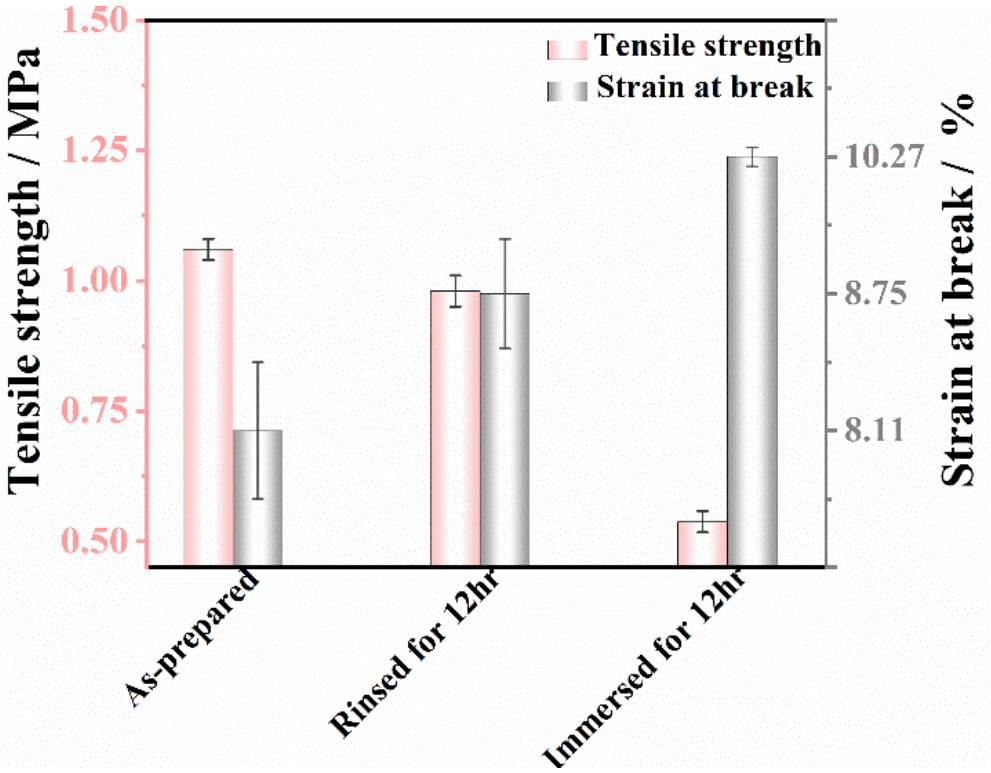

Fig. S4. Statistical data for the mechanical properties of as-prepared G0.6-T0.6, G0.6-T0.6-U0.12 rinsed for 12 hr, and G0.6-T0.6-U0.12 immersed for 12 hr.

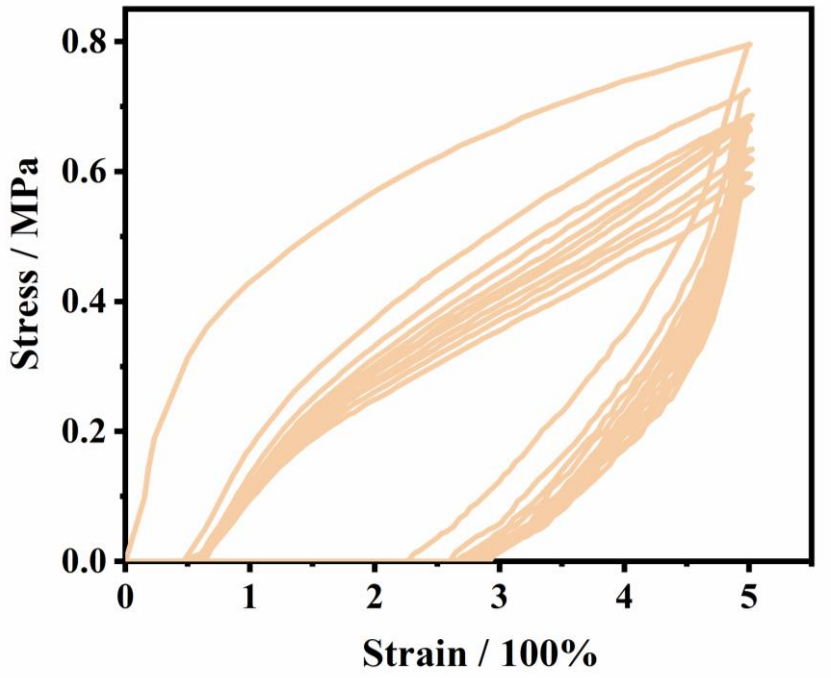

Fig. S5. Cyclic tensile test of G0.6-T0.6 to a maximum tensile strain of 5.

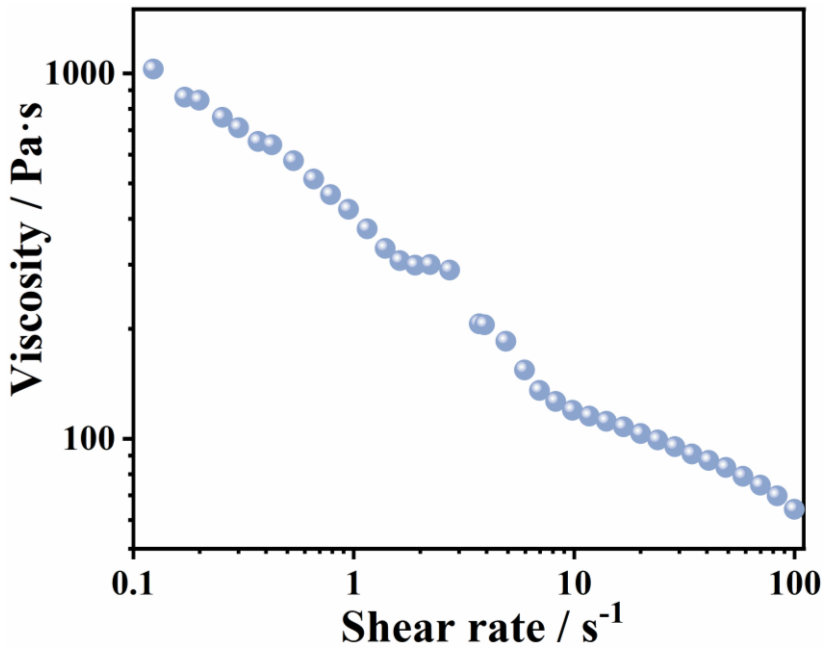

Fig. S6. The shear-thinning property of G0.6-T0.6-U0.12 at ambient temperature (25 ºC).

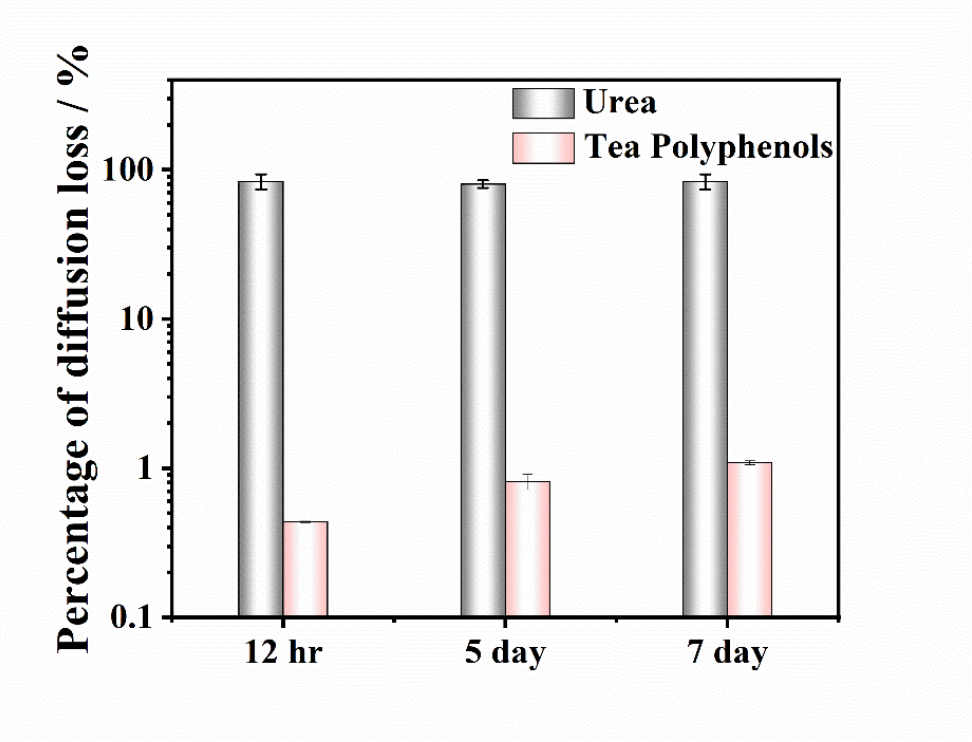

Fig. S7. The loss of tea polyphenols through diffusion from G0.6-T0.6-U0.12 in water was measured, which was negligible in comparison with that of urea in this study. After 12 hr, the loss of urea molecules reached 83.6% (molar ratio). In contrast, after 7 days, the loss of TP molecules was only 1.1% (molar ratio).

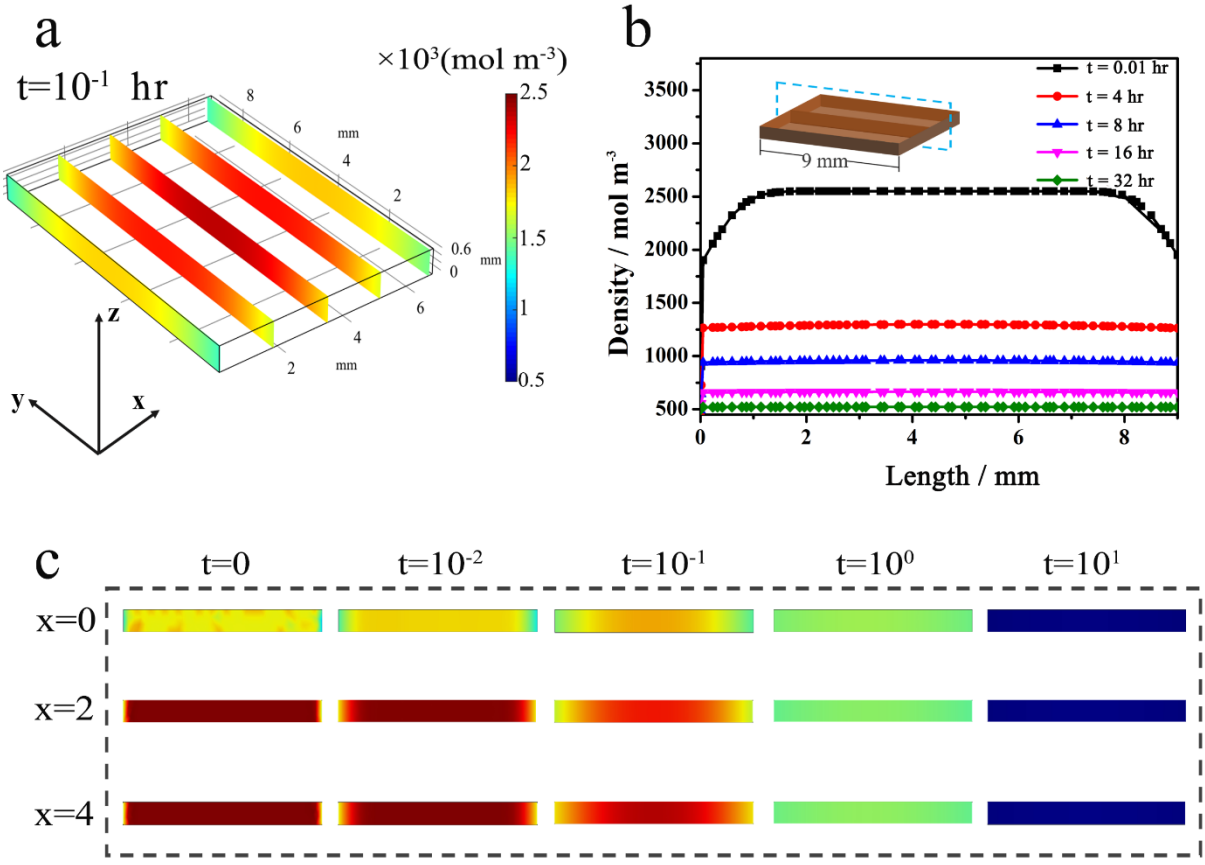

Fig. S8. a Spatial distributions of urea (in molar concentration) on the specific cross sections at the moment of t=0.1 hr. **b** Spatial distributions of average molar concentrations on the cross sections along the long sides at different time points. **c** Spatial distributions of urea (in molar concentration) at the specific cross sections along the long sides at different time points of t= t=0, 0.01, 0.1, 1, 10 and 100 hr, respectively.

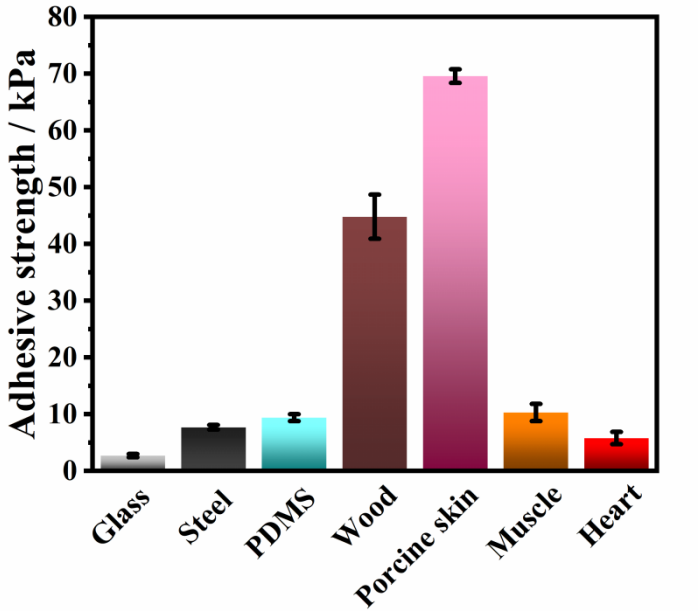

Fig. S9. In-air adhesion of G0.6-T0.6-U0.12 to multiple substrates.

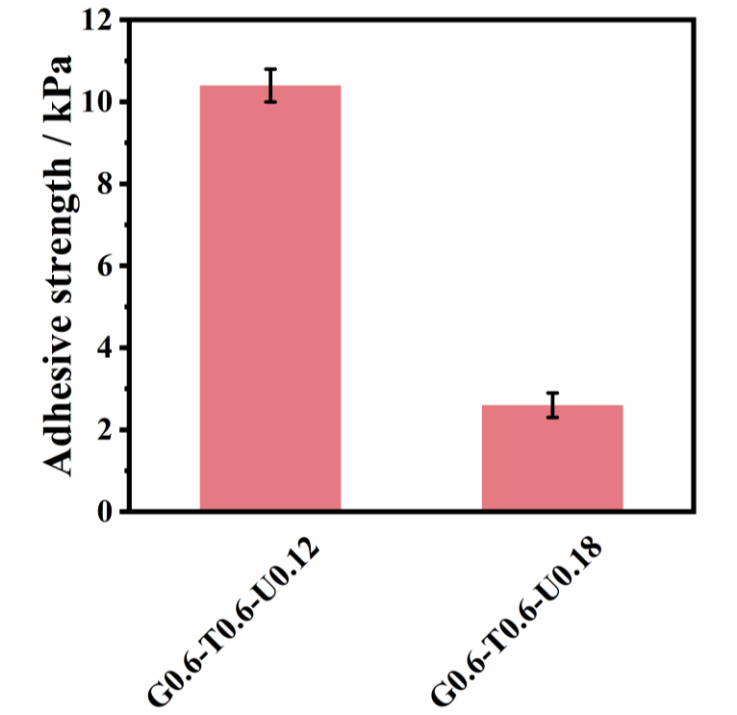

Fig. S10. The 10 sec' underwater adhesive strength to porcine skin of G0.6-T0.6-U0.12 and G0.6-T0.6-U0.18.

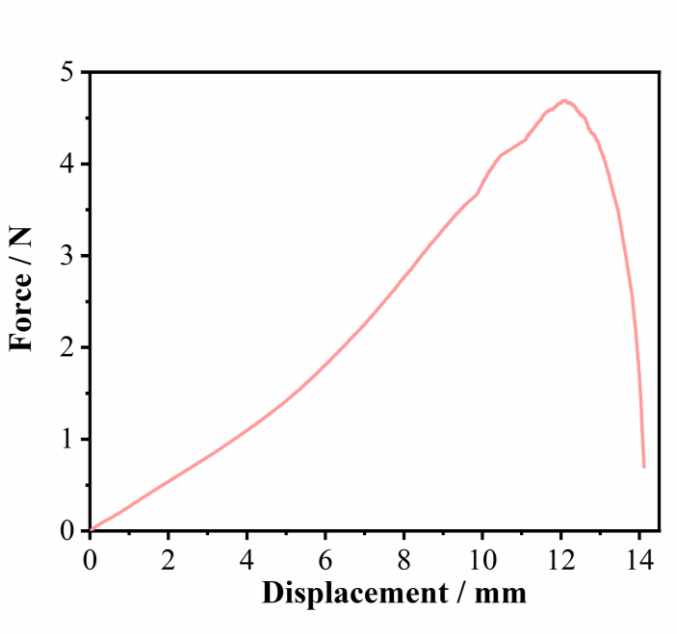

Fig. S11. The representative curve for the lap-shear test on the underwater adhered porcine skin after 8 hrs' immersion in water. The measured bonding area for this test was 5×6 mm^2. The corresponding adhesive strength for this test was calculated to be 156.4 kPa.

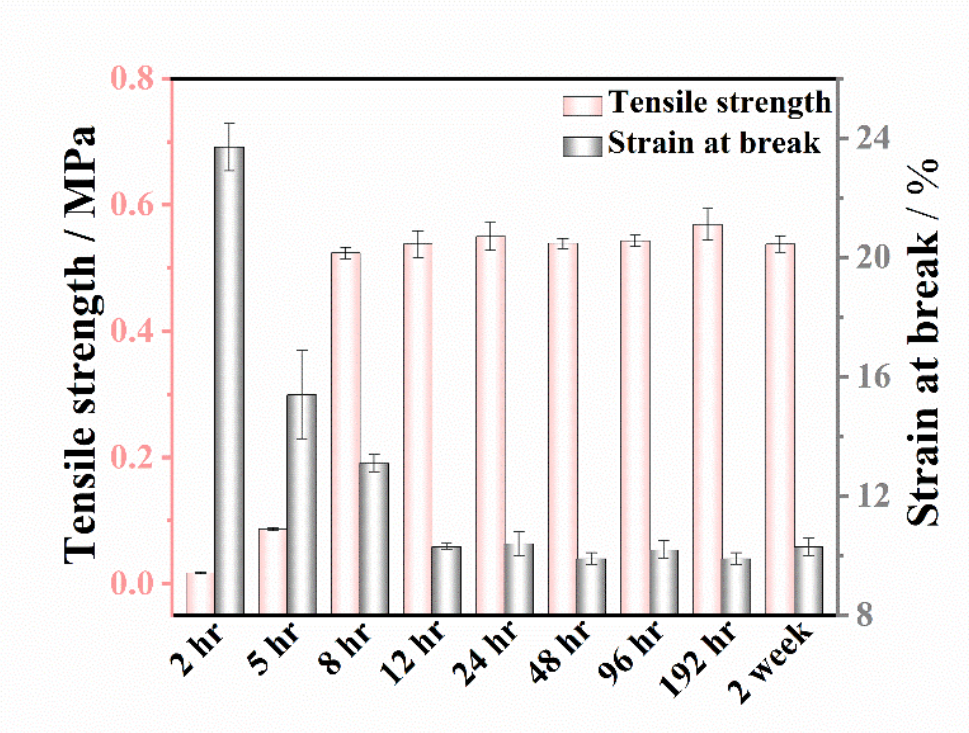

Fig. S12. The tensile strength and strain at break of G0.6-T0.6-U0.12 in different time intervals after immersion.

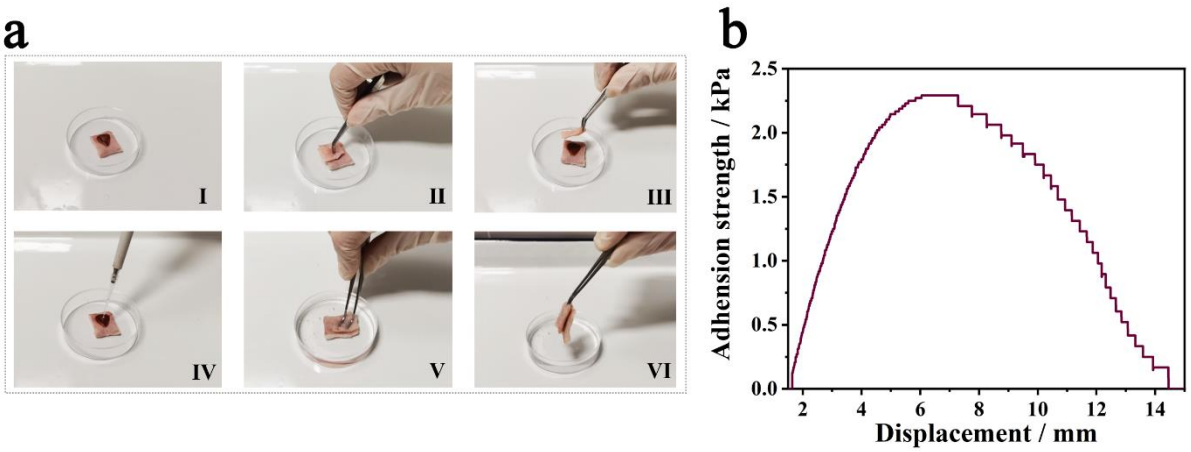

Fig. S13. a The formation of the "non-adhesive interface" and the regeneration of the "adhesive interface". **I.** The "non-adhesive interface" formed on top of a piece of porcine skin following the same method mentioned in **Fig. 4a** in the main text. **II.** Another piece of porcine skin was pressed onto the "non-adhesive interface" for 10 sec in air. **III.** There was no adhesion to the piece of porcine skin placed on it. **IV.** The "non-adhesive interface" was smeared with 10 μl urea solution (1 mol L^{-1}). **V.** After 4 hr, another piece of porcine skin was pressed on the top for 10 sec under water. **VI.** Obvious underwater adhesiveness appeared, confirming the transformation of the "non-adhesive interface" into the "adhesive interface". **b** The corresponding lap-shear adhesive test was conducted and the curve was presented.

If the already formed "non-adhesive interface" of the hydrogel was immersed in the urea solution (1 mol L^{-1}), the "non-adhesive interface" remained non-adhesive in water and the hydrogel gradually degraded because excessive urea molecules in the solution dissociated the GE-TP hydrogen bonds. Nevertheless, if the "non-adhesive interface" was treated with 10 μl urea solution in air, the "non-adhesive interface" turned into the "adhesive interface" after 4 hr. The corresponding 10 sec' underwater adhesive strength to porcine skin was 2.3 kPa.

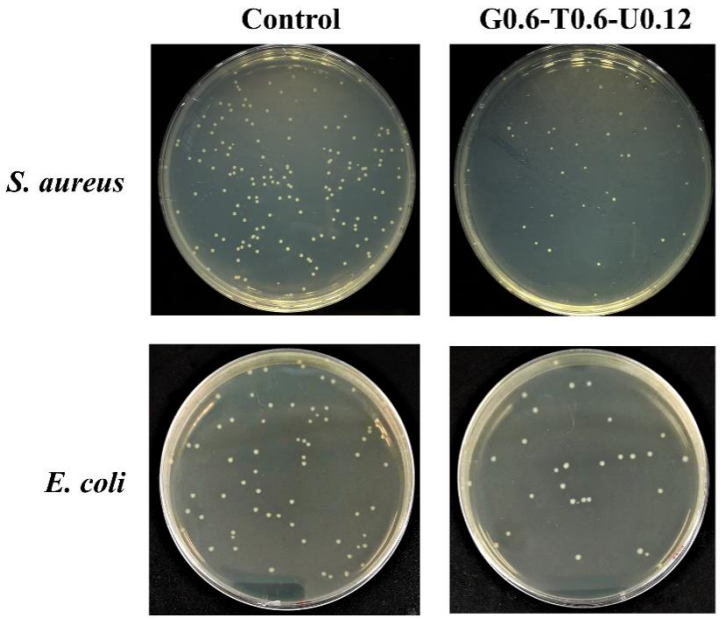

Fig. S14. Antibacterial properties of the G0.6-T0.6-U0.12 hydrogel against *S. aureus* or *E. coli*.

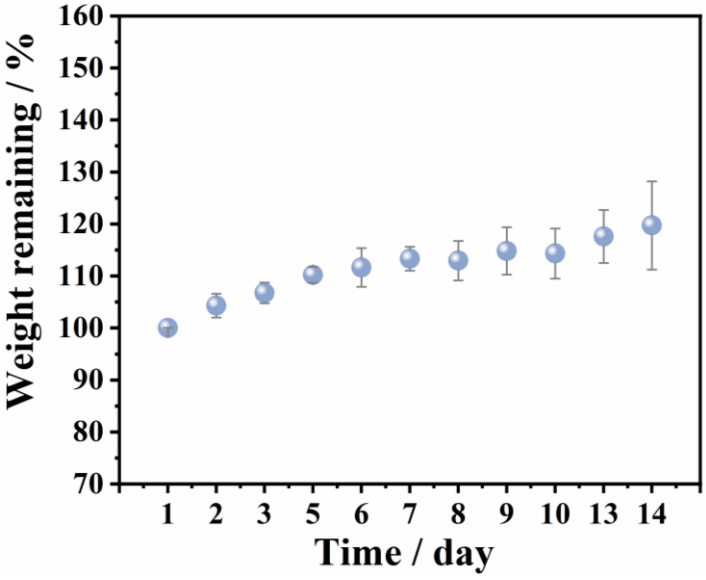

Fig. S15. The evaluation on the degradation of G0.6-T0.6-U0.12 in the distilled water at ambient temperature.

Supplementary Tables

Table S1. Composition of the samples

Samples	GE (g)	TP (g)	Urea (g)
G0.6-DA0.6[a]	0.6	0	0
G0.6-TA0.6[b]	0.6	0	0
G0.6-T0.6	0.6	0.6	0
G0.6-T0.3[c]	0.6	0.3	0
G0.6-T0.9[d]	0.6	0.9	0
G0.6-T0.6-U0.06	0.6	0.6	0.06
G0.6-T0.6-U0.12[e]	0.6	0.6	0.12
G0.6-T0.6-U0.18	0.6	0.6	0.18

[a] 0.6g dopamine (DA) was used instead of tea polyphenols (TP) for G0.6-DA0.6, which failed to reach gelation because of the relatively weak hydrogen bonding between polydopamine and gelatin (GE).[16]

[b] 0.6g tannic acid (TA) was used instead of tea polyphenols (TP) for G0.6-TA0.6, which gave rise to flocculent precipitation. The hydrogel bonding between GE and TA were too strong to derive bulk remoldable hydrogel via simple mixing under mild conditions.[17, 18]

[c, d] We tried to incorporate GE with different amount of TP. However, excessive sticky GE was left after synthesising G0.6-T0.3. And excessive brown TP was left after synthesising G0.6-T0.9. Only in the case of G0.6-T0.6, there was no obvious residue but water left after synthesis. The as-prepared "G0.6-T0.3" and "G0.6-T0.9" samples seemed identical to G0.6-T0.6. And they displayed similar mechanical properties as those of G0.6-T0.6, indicating their similar chemical composition.[17-19] Therefore, G0.6-T0.6 was investigated in detail in this work, instead of G0.6-T0.3 or G0.6-T0.9.

[e] G0.6-T0.6-U0.12 was marked in blue color because of its superior properties comparing to G0.6-T0.6-U0.06 and G0.6-T0.6-U0.18. Comparing to G0.6-T0.6-U0.12, G0.6-T0.6-U0.06 was not injectable, while G0.6-T0.6-U0.18 had inferior mechanical properties. As seen in **Fig. S10**, the 10 sec' underwater adhesive strength to porcine skin of G0.6-T0.6-U0.18 was significantly lower than that of G0.6-T0.6-U0.12. So, this work mainly focused on G0.6-T0.6-U0.12, unless otherwise specified.

Table S2. Comparison of properties for the existing adhesive gels. (Note that the symbols of '√' and '--' denote 'Yes' and 'No or N/A', respectively.)

Adhesive gels	Injectable (post-crosslinking condition)	Tensile strength / kPa	Time to achieve firm adhesion in air and/or under water (substrate)	In-air adhesive (adhesive strength, adhesive testing method, substrate)	Underwater adhesive (adhesive strength, adhesive testing method, substrate, durability)	Adjustable adhesive/non-adhesive interfaces (condition)
THIS WORK	√ (water)	1010	10 sec	√ (69.6 kPa, shear, porcine skin)	√ (152.9 kPa, shear, porcine skin, > 2 weeks)	√ (water)
Zhao Q, et al. Nat. Mater. 2016[20]	√ (water)	--	25 sec	--	√ (2 J m^{-2}, adhesion force measurements, glass, > 1 hr)	--
Rao P, et al. Adv.Mater.2018[21]	--	400	10 sec	√ (25 kPa, tensile, glass)	√ (7 kPa, tensile, porcine pericardial, --)	--
Fan HL, et al. Adv.Funct.Mater.2020[22]	--	1000	10 sec	--	√ (180 kPa, shear, negatively charged glass, > 100 days)	--
Cui CY, et al. Adv.Mater.2019[23]	√ (water)	--	10 sec	--	√ (390 kPa, shear, iron sheet, > 72 hr)	--
Han L, et al. Adv.Funct.Mater.2019[24]	--	15	120 sec	√ (55 kPa, shear, glass)	√ (75 kPa, tensile, glass, > 7 days)	--
Fan HL, et al. Nat.Commun.2019[25]	√ (seawater)	500	10 sec	--	√ (60 kPa, tensile, glass in seawater, --)	--
Ju GN, et al. Angew.Chem.Int.Ed.2018[26]	--	--	5 min	--	√ (386 N m^{-2}, shear, PDDA, --)	--
Yuk H, et al. Nature.2019[27]	--	60	5 sec	√ (120 kPa, shear, porcine skin)	--	--
Liu BC, et al. Biomaterials.2018[7]	--	160	1 min	√ (81 kPa, shear, porcine skin)	--	--
Fan HL, et al. Macromolecules.2018[28]	--	9500	2 min	√ (70 kPa, shear, porcine skin)	--	--
Su X, et al. Mater.Horiz.2020[2]	--	48.6	10 sec	√ (63.3 kPa, shear, porcine skin)	√ (18.7 kPa, shear, porcine skin, > 24 hr)	--
Fan XM, et al. Mater.Horiz.2020[29]	--	570	20 sec	√ (187.1 kPa, shear, porcine skin)	√ (--, --, porcine skin, > 8 hr)	√ (base or metal ion treatment)
Hong Y, et al. Nat.Commun.2019[30]	√ (UV radiation)	--	< 20 sec	√ (80 kPa, peel, wet sausage skin)	--	--
Lang N, et al. Sci.Transl.Med.2014 (cyanoacrylate)[31]	√ (--)	--	5 sec (bovine pericardium)	√ (1 kPa, tensile, wet bovine pericardium) (38 kPa, tensile, fresh bovine pericardium)	--	--
Lang N, et al. Sci.Transl.Med.2014 (Fibrin sealant)[31]	√ (--)	--	5 sec (bovine pericardium)	√ (15 kPa, tensile, wet bovine pericardium) (20 kPa, tensile, fresh bovine pericardium)	--	--
Zhao X, et al. Biomaterials.2017[32]	√ (--)	--	3 hr (porcine skin)	√ (4.9 kPa, shear, porcine skin)	--	--
Wang R, et al. Adv.Funct.Mater.2017[33]	√ (H_2O_2 oxidation)	--	30 min (porcine skin)	√ (147 kPa, shear, porcine skin)	--	--
Lu XL, et al. Biomaterials.2020[34]	√ (MgO oxidation)	4500	2 hr (porcine skin)	√ (127 kPa, shear, porcine skin)	--	--
Qu J, et al. Biomaterials.2018[35]	√ (--)	--	3 hr (porcine skin)	√ (6.1 kPa, shear, porcine skin)	--	--
Zhao X, et al. Adv.Funct.Mater.2020[36]	√ ($FeCl_3$ treatment & pH adjustment)	--	3 hr (porcine skin)	√ (5.2 kPa, shear, porcine skin)	--	--
Li SD, et al. Adv.Funct.Mater.2020[37]	√ (pH adjustment)	--	10 min (collagen casting)	√ (15 kPa, shear, porcine skin)	--	--
Ma YF, et al. Adv.Funct.Mater.2020[38]	√ (UV radiation)	--	10 sec (heart)	√ (97.65 kPa, shear, porcine skin)	--	--
Xie T, et al. Mater.Horiz.2020[39]	√ ($FeCl_3$ treatment)	--	10 min (porcine skin)	√ (11 kPa, shear, porcine skin)	--	√ (zinc ion treatment)
Cui CY, et al. Adv.Funct.Mater.2020[40]	--	60	5 sec (porcine skin)	√ (367 J m^{-2}, peel, porcine skin)	√ (208 J m^{-2}, peel, porcine skin, > 8hr)	√ (cationic polymer solution treatment)
Chen XY, et al. Proc. Natl. Acad. Sci. U.S.A. 2020[41]	--	--	5 sec (porcine skin)	√ (400 J m^{-2}, peel, wet porcine skin)	--	√ ($NaHCO_3$ and glutathione treatment)
Wang SH, et al. Adv.Funct.Mater.2020[42]	--	--	0.5 sec (glass)	√ (14 kPa, pressure sensing, glass)	√ (14 kPa, pressure sensing, glass)	√ (magnetic field)

Supplementary Videos

Video S1: The spatio-temporal dynamics of water-triggered urea diffusion in the G0.6-T0.6-U0.12 hydrogel sample and on the adhesion interface between the hydrogel and the porcine skin.

Video S2: The G0.6-T0.6 hydrogel was non-adhesive to either glass or porcine skin in water.

Video S3: The injectable G0.6-T0.6-U0.12 hydrogel was efficiently adhesive to either glass or porcine skin in water.

Video S4: The formation of "non-adhesive" interface for G0.6-T0.6-U0.12 after 1 hr's immersion in water.

Video S5: The underwater 3D printing of G0.6-T0.6-U0.12 patterns onto glass or porcine skin

Video S6: The stability of the underwater 3D printed logos on glass or porcine skin against shaking and flushing.

Video S7: The blowing G0.6-T0.6-U0.12 hydrogel balloon by using a thin syringe needle.

References

1. L. Han, L. W. Yan, K. F. Wang, L. M. Fang, H. P. Zhang, Y. H. Tang, Y. H. Ding, L. T. Weng, J. L. Xu, J. Weng, Y. J. Liu, F. Z. Ren and X. Lu, *NPG Asia Mater.*, 2017, **9**, 12.
2. X. Su, Y. Luo, Z. Tian, Z. Yuan, Y. Han, R. Dong, L. Xu, Y. Feng, X. Liu and J. Huang, *Mater. Horiz.*, 2020, **7**, 2651-2661.
3. M. Zhang, R. Guo, K. Chen, Y. Wang and Y. Zhang, *Proc. Nat. Acad. Sci. U. S. A.*, 2020, **117**, 202003079.
4. Z. Wang, L. Chen, Y. Chen, P. Liu, H. Duan and P. Cheng, *Research*, 2020, **2020**, 1426078.
5. V. Rubentheren, T. A. Ward, C. Y. Chee and C. K. Tang, *Carbohydr. Polym.*, 2015, **115**, 379-387.
6. V. Rubentheren, T. A. Ward, C. Y. Chee, P. Nair, E. Salami and C. Fearday, *Carbohydr. Polym.*, 2016, **140**, 202-208.
7. B. Liu, Y. Wang, Y. Miao, X. Zhang, Z. Fan, G. Singh, X. Zhang, K. Xu, B. Li, Z. Hu and M. Xing, *Biomaterials*, 2018, **171**, 83-96.
8. R. Usha and T. Ramasami, *Thermochim. Acta*, 1999, **338**, 17-25.
9. S. Kashiwagi, K. Nakamura, K. Takeo, T. Takasago, A. Uchimichi and H. Ito, *Electrophoresis*, 1991, **12**, 420.
10. B. Laura, *Nutr. Rev.*, 1998, **56**, 317-333.
11. M. Sun, H. Guo, J. Zheng, Y. Wang and X. Jia, *Polym. Test.*, 2020, **91**, 106831.
12. H. N. Graham, *Prev. Med.*, 1992, **21**, 334-350.
13. B. H. Cipriano, S. J. Banik, R. Sharma, D. Rumore, W. Hwang, R. M. Briber and S. R. Raghavan, *Macromolecules*, 2014, **47**, 4445-4452.
14. G. R. Gao, G. L. Du, Y. N. Sun and J. Fu, *ACS Appl. Mater. Interfaces*, 2015, **7**, 5029-5037.
15. X. Su, S. Mahalingam, M. Edirisinghe and B. Chen, *ACS Appl. Mater. Interfaces*, 2017, **9**, 22223-22234.
16. C. J. Fan, J. Y. Fu, W. Z. Zhu and D. A. Wang, *Acta Biomaterialia*, 2016, **33**, 51-63.
17. S. Yang, Y. Zhang, T. Wang, W. Sun and Z. Tong, *ACS Appl. Mater. Interfaces*, 2020, **12**, 46701-46709.

18. Z. Ahmadian, A. Correia, M. Hasany, P. Figueiredo and M. A. Shahbazi, *Adv. Healthc. Mater.*, 2021, **10**, 2001122.
19. Q. Zhao, S. Mu, Y. Long, J. Zhou, W. Chen, D. Astruc, C. Gaidau and H. Gu, *Macromol. Mater. Eng.*, 2019, **304**, 1800664.
20. Q. Zhao, D. W. Lee, B. K. Ahn, S. Seo, Y. Kaufman, Jacob N. Israelachvili and J. H. Waite, *Nat. Mater.*, 2016, **15**, 407-412.
21. P. Rao, T. L. Sun, L. Chen, R. Takahashi, G. Shinohara, H. Guo, D. R. King, T. Kurokawa and J. P. Gong, *Adv. Mater.*, 2018, **30**, 1801884.
22. H. Fan, J. Wang and J. P. Gong, *Adv. Funct. Mater.*, 2020, 2009334.
23. C. Cui, C. Fan, Y. Wu, M. Xiao, T. Wu, D. Zhang, X. Chen, B. Liu, Z. Xu and B. Qu, *Adv. Mater.*, 2019, **31**, 1905761.
24. L. Han, M. Wang, L. O. Prieto-López, X. Deng and J. Cui, *Adv. Funct. Mater.*, 2020, **30**, 1907064.
25. H. Fan, J. Wang, Z. Tao, J. Huang, P. Rao, T. Kurokawa and J. P. Gong, *Nat. Commun.*, 2019, **10**, 5127.
26. G. Ju, M. Cheng, F. Guo, Z. Qian and S. Feng, *Angew. Chem. Int. Ed.*, 2018, **57**, 8936.
27. H. Yuk, C. E. Varela, C. S. Nabzdyk, X. Mao, R. F. Padera, E. T. Roche and X. Zhao, *Nature*, 2019, **575**, 169-174.
28. H. Fan, J. Wang and Z. Jin, *Macromolecules*, 2018, **51**, 1696-1705.
29. X. Fan, Y. Fang, W. Zhou, L. Yan, Y. Xu, H. Zhu and H. Liu, *Mater. Horiz.*, 2021, **8**, 997-1007.
30. Y. Hong, F. Zhou, Y. Hua, X. Zhang, C. Ni, D. Pan, Y. Zhang, D. Jiang, L. Yang, Q. Lin, Y. Zou, D. Yu, D. E. Arnot, X. Zou, L. Zhu, S. Zhang and H. Ouyang, *Nat. Commun.*, 2019, **10**, 2060.
31. N. Lang, M. J. N. Pereira, Y. Lee, I. Friehs, N. V. Vasilyev, E. N. Feins, K. Ablasser, E. D. Ocearbhaill, C. Xu and A. Fabozzo, *Sci. Transl. Med.*, 2014, **6**, 218.
32. X. Zhao, H. Wu, B. Guo, R. Dong, Y. Qiu and P. X. Ma, *Biomaterials*, 2017, **122**, 34-47.
33. R. Wang, J. Li, W. Chen, T. Xu, S. Yun, Z. Xu, Z. Xu, T. Sato, B. Chi and H. Xu, *Adv. Funct. Mater.*, 2017, **27**, 1604894.
34. X. Lu, S. Shi, H. Li, E. Gerhard, Z. Lu, X. Tan, W. Li, K. M. Rahn, D. Xie, G. Xu, F. Zou, X. Bai, J. Guo and J. Yang, *Biomaterials*, 2020, **232**, 119719.
35. J. Qu, X. Zhao, Y. Liang, T. Zhang, P. Ma and B. Guo, *Biomaterials*, 2018, **183**, 185-199.
36. X. Zhao, Y. Liang, Y. Huang, J. He, Y. Han and B. Guo, *Adv. Funct. Mater.*, 2020, **30**, 1910748.
37. S. Li, N. Chen, X. Li, Y. Li, Z. Xie, Z. Ma, J. Zhao, X. Hou and X. Yuan, *Adv. Funct. Mater.*, 2020, **30**, 2000130.
38. Y. Ma, J. Yao, Q. Liu, T. Han, J. Zhao, X. Ma, Y. Tong, G. Jin, K. Qu, B. Li and F. Xu, *Adv. Funct. Mater.*, 2020, **30**, 2070259.
39. T. Xie, J. Ding, X. Han, H. Jia, Y. Yang, S. Liang, W. Wang, W. Liu and W. Wang, *Mater. Horiz.*, 2020, **7**, 605-614.
40. C. Cui, T. Wu, X. Chen, Y. Liu, Y. Li, Z. Xu, C. Fan and W. Liu, *Adv. Funct. Mater.*, 2020, **30**, 2005689.
41. X. Chen, H. Yuk, J. Wu, C. S. Nabzdyk and X. Zhao, *Proc. Nat. Acad. Sci. U. S. A.*, 2020, **117**, 202006389.
42. S. Wang, H. Luo, C. Linghu and J. Song, *Adv. Funct. Mater.*, 2020, **31**, 2009217.